Tikrit Journal of Pure Science 21 (6) 2016 *ISSN: 1813 – 1662 (Print)*
E-ISSN: 2415 – 1726 (On Line)

Synthesis of Nickel Ferrite $NiFe_2O_4$ Nanoparticles/PVA composite and studying Its electric properties

Ibrahim F. waheed[1], Emaad T. Bakir[1], Sabah M. Ali[2]
[1] *Department of chemistry , College of Science, Tikrit University, Tikrit , Iraq.*
[2] *Department of Physics , College of Education For Pure Science, Kirkuk University , Kirkuk , Iraq.*
imaofs83@yahoo.com , emaad_bakir@yahoo.com , sabah_yagmur@yahoo.com

Abstract
In this work focused on preparing Nickel Ferrite $NiFe_2O_4$ Nanoparticles (NFNPs) which prepared by Sol-Gel Auto-Combustion Method. Incorporating (NFNPs) in PVA afforded NFNPs/PVA composites with different weight of NFNPs. the NFNPs /PVA composite and pure PVA were identified by different techniques, FTIR measurements, The scanning electron microscope (SEM), and powder x-ray diffraction. The electrical properties of the NFNPs/PVA composite was investigated. These properties include dielectric constant, permittivity(ε'), imaginary permittivity(ε"), conductivity (σ_{Ac}) and loss factor (tan δ). The measurements were performed at frequencies (5000Hz-1MHz) at room temperature.
Key words: Nickel Ferrite, x-ray diffraction, dielectric constant.

1. Introduction

A ferrite is a type of ceramic compound composed of iron oxide (Fe_2O_3) combined chemically with one or more additional metallic elements. The spinel ferrite structure $MeFe_2O_4$, where Me refers to the metal, can be described as a cubic close-packed arrangement of oxygen atoms, with Me^{2+} and Fe^{3+} at two different crystallographic sites. These sites have tetrahedral and octahedral oxygen coordination (termed as A and B-sites, respectively), so the resulting local symmetries of both sites are different. The spinel structure contains two cation sites for metal cation occupancy. There are 8 A-sites in which the metal cations are tetrahedrally coordinated with oxygen, and 16 B-sites which possess octahedral coordination. When the A-sites are occupied by Me^{2+} cations and the B-sites are occupied by Fe^{3+} cations, the ferrite is called a normal spinel. If the A-sites are completely occupied by Fe^{3+} cations and the B-sites are randomly occupied by $Me^{2+}$and Fe^{3+}cations, the structure is referred to as an inverse spinel. In most spinels, the cation distribution possesses an intermediate degree of inversion where both sites contain a fraction of the Me^{2+} and Fe^{3+} cations. Magnetically, spinel ferrites display ferrimagnetic ordering. The magnetic moments of cations in the A and B-sites are aligned parallel with respect to one another. Between the A and B-sites the arrangement is antiparallel and as there are twice as many B-sites as A-sites, there is a net moment of spins yielding ferrimagnetic ordering for the crystal. The choice of metal cation and the distribution of ions between the A and B-sites therefore, offer a tunable magnetic system [1-3]. Spinel ferrite material with $MeFe_2O_4$ type (Me: Fe, Co, and Ni) is group of magnetic materials that have excellent electromagnetic properties so much applied in information storage technology, diagnosis medical, heating and cooling using a magnetic material, anode on the battery, and catalysis [4,5].

2. Experimental Part

2.1 Materials

The starting materials used were obtained from different sources and companies like nickel nitrate hexahydrated and ferric nitrate nanohydrated (CDH co.), Citric acid (ALPHA co.), Ammonium hydroxide (Fluka co.), Poly(vinylalcohol) (PVA) (AFCO co.)

2.2 Preparation of Nickel Ferrite $NiFe_2O_4$ Nanoparticles (NFNPs)

The sol - gel method is widely used in synthesis of ferrite nanocrystals because of its high reaction rate, low preparation temperature, and production of small particles. Hence, in present experiment, $NiFe_2O_4$ nanoparticles were synthesised via a sol-gel route as described in the literature [6-8]. In terms of the atomic ratio n(Ni)/ n(Fe)=1: 2, The synthesis scheme of nanostructural Figure 1. In a typical reaction (1.164 g; 4 mmol) of nickel nitrate hexahydrated $Ni(NO_3)_2.6H_2O$ (crystal-shaped dark green) was dissolved in 25 ml of distilled water and, separately, (3.232 g; 8 mmol) of ferric nitrate nanohydrated $Fe(NO_3)_3.9H_2O$ (in the form of white crystals) was dissolved in 50 ml of distilled water. The solutions were mixed and added slowly to a solution of (2.304 g) of citric acid and were dissolved into an aqueous. The ammonia solution was added into the solution to adjust the pH value to 7 and stabilize the nitrate-citrate solution. During this procedure, the solution was continuously stirred using a magnetic agitator and kept at a temperature of 50 °C. Then , the mixed solution was poured into a vessel , heated slowly to 90-95°C and stirred constantly until it became viscous and color changed as the solution turned into a green porous dry gel. The dried gel was completely burnt out to form a loose powder and then submitted to calcinations at 550°C for 2.5 h in furnace, finally yielding $NiFe_2O_4$ nanoparticles.

2.3 Fabrication of NFNPs/PVA composites

Polymeric nano Composites films of different weight percent concentrate-ions are prepared. These films contain different proportions of NFNPs was added to the PVA solutions (25ml) Then, mixture exposed to sonication for 10-15 min to ensure dispersion of the nanosheets between the polymer chains, after the sonication, and mixed by magnetic stirrer for few seconds. Then, the mixture was poured into the

specific glass mold and left overnight. Then, the film was peeled out and dried under vacuum for 4 hours,to obtain dry films.

2.4. Characterization

Fourier transform infrared spectroscopy (FT-IR) measurements were carried out by using a shimadzu 8400 spectrophotometer over the range of 4000-400 cm^{-1}. Scanning electron microscope (SEM) observation was performed on a Hitachi S-4700 microscope with an accelerating voltage of 20 kV. Transmission electron microscope. X-ray diffraction (XRD) analysis was carried out with a Rigaka D/max 2500 diffractometer using a Cu Ka radiation source.

Dielectric properties of the RGS/PVA composites were measured by using LCR meter type PM6036. were studied by measurement of real, imaginary permittivity, loss factor (tan δ) and the Ac conductivity (σ_{Ac}). The investigations were made at different frequencies (5000Hz-1MHz) at room temperature.The dielectric parameter as a function of frequency is described by the complex permittivity

$$\varepsilon^*(\omega) = \varepsilon'(\omega)-\varepsilon''(\omega) \quad \ldots.(1)$$

where the real part ε' and imaginary part ε'' are the components for the energy storage and energy loss, respectively, in each cycle of the electric field. (ω) is the angular frequency; $\omega=2\pi f$, f is applied frequency. The measured capacitance, C was used to calculate the dielectric constant, ε' using the following expression.

$$\varepsilon' = Cd/\varepsilon_\circ A \ldots. (2)$$

where d is the thickness between the two electrodes (film thickness), A is the area of the electrodes, $\varepsilon_\circ$ is permittivity of the free space, $\varepsilon_\circ = 8.85*10^{-12}$ $F.m^{-1}$ and whereas for dielectric loss $\varepsilon''(\omega)$, and tanδ is tangent delta[9]:

$$\varepsilon''(\omega) = \varepsilon'(\omega) \,.\, tan\delta(\omega) \quad \ldots..(3)$$

The AC conductivity (σ_{ac}) can be calculated by the following equation[9]:

$$\sigma = \varepsilon_\circ \varepsilon' \omega \, tan\delta \quad \ldots..(4)$$

3. Results and discussion

Fig.1 shows the FT-IR spectra of as-Gel $NiFe_2O_4$ and those calcined at various temperatures. In the case of as-gel, as shown in Fig.1a, various types of functional groups such as broad band centered between (3419-3034)cm^{-1}corresponded to O-H stretching of hydroxyl group and a stretching mode of H_2O molecules [10]. the peaks around (2850 and 2816) cm^{-1} can be assigned to the asymmetric and symmetric vibrations of ν(C-H), respectively, at (1766)cm^{-1} for the ν(C=O) moiety of (-COOH) groups of citric acid. there are special absorption peaks appearing at (1614 and 1384)cm^{-1}, which correspond to the carboxylate anion, and anti-symmetric NO_3 stretching vibrations, respectively[11]. The band at (1076)cm^{-1} are ascribed to alkoxy stretching. absorption peak appearing at (648)cm^{-1} which correspond to ν(Fe-O).

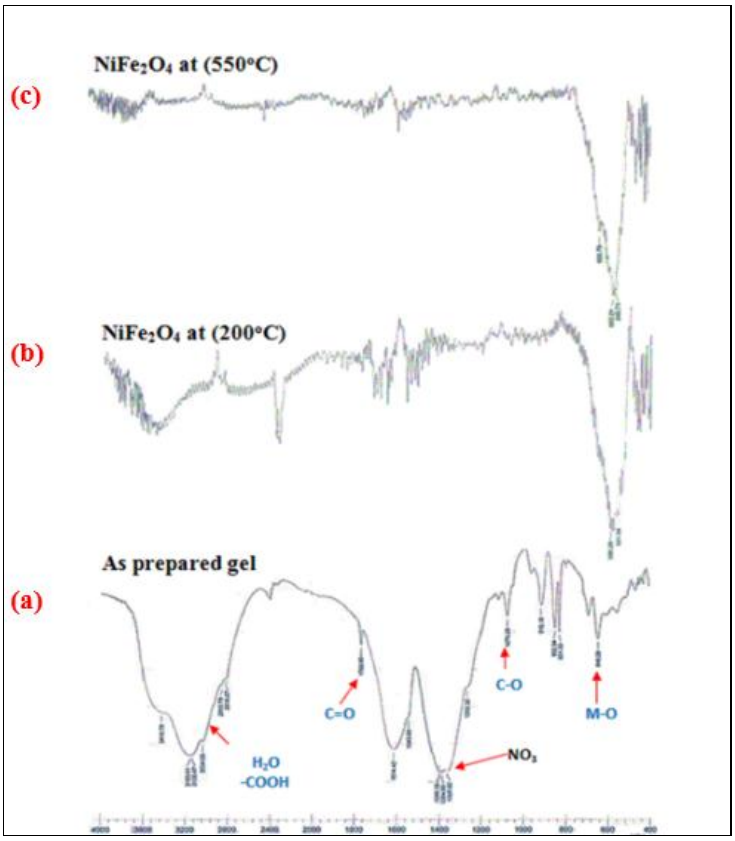

Fig.1 FTIR spectra of NFNPs (a) as gel (b) calcined at 200°C (c) calcined at 550°C

The decomposition of hydroxide to oxide phase for the formation of spinel ferrites were well reflected in the FTIR spectra when calcined[11]. Where after calcination at 550°C as shown in Fig.1c the remaining two weak peaks lies in region (1560 and 2364) cm^{-1} are due to the stretching vibrations between octahedral metal ions and oxygen ions Hence the two strongest peaks confirmed the spinel structure of $NiFe_2O_4$ in region (628 and 549)cm^{-1} according to Waldron [12,13].the high frequency band υ_1 around (628)cm^{-1} is attributed to that of tetrahedral complexes. The band υ_2 around (549)cm^{-1} corresponding to octahedral complexes. The variation in the band positions is due to the difference in the (Fe^{3+}–O^{2-}) distances for the octahedral and tetrahedral complexes. The tetrahedral cluster has shorter bond lengths and the octahedral cluster has longer bond lengths[14].

The crystal structure and phase purity of $NiFe_2O_4$ calcined at 200°C and 550°C was characterized by XRD Fig.2. It shows that the sharp crystalline peaks observed for sample calcined above 550°C. The peaks appearing at 2θ values 18.52°, 30.42 °, 35.79°, 37.463°, 43.501°, 54.18, 57.5°, and 63.108° may be assigned for X-ray scattering from the (111) (220) (311) (222) (400) (422) (511) and (440) planes of the spinel crystal lattice, respectively, which confirm the presence of single phase $NiFe_2O_4$ with a face-centered cubic structure [15]. Except for the impure phase of α-Fe_2O_3, which is found in all calcined samples and occurs naturally as hematite [16]. the remaining peaks correspond to the standard pattern of $NiFe_2O_4$ (cubic, a =8.319332 Å , space group: Fd3m, volume cell (575.791647Å), ICDD PDF: 44-1485) The obtained values of lattice constants for $NiFe_2O_4$ at 550°C were in good agreement with the standard ICDD cards file No.(96-591-0065) data file as well as that of reported values. In thermal treatment method, the optimum temperature for the calcination of nickel ferrite nanoparticles was 550°C because this temperature was the minimum temperature at which the nanoparticles were pure; also, this was the temperature at which the nanoparticles had the smallest particle size and a nearly uniform distribution of shapes[17]. The average crystallite size has been evaluated from the full width at half maximum of the reflection (311) peak in the XRD pattern. It is important to note that, The crystallite size was observed to increase with higher sintering temperatures. It has been reported that the sintering process generally decreases lattice defects and strain but this technique can cause the coalescence of smaller grains, resulting in an increased average grain size for the nanoparticles [18-20].

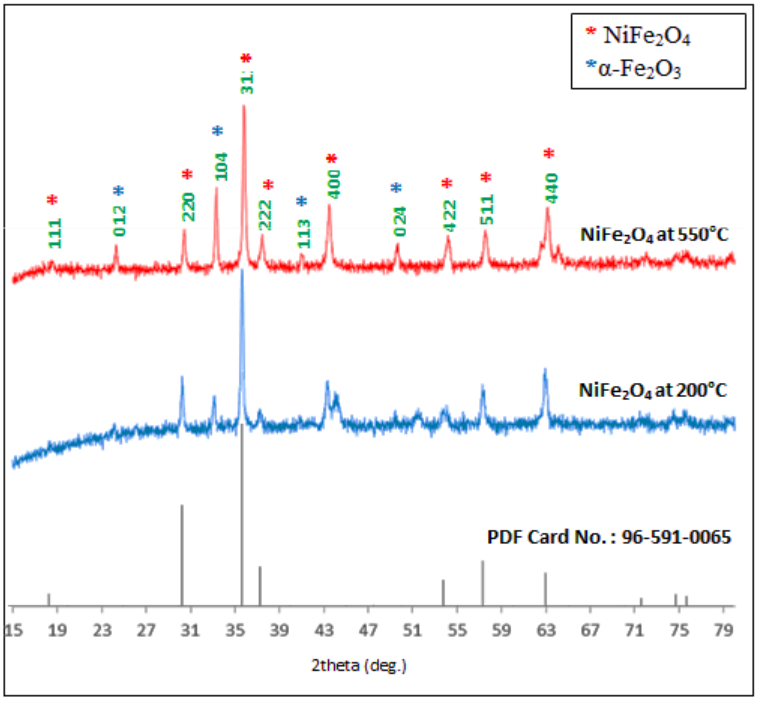

Fig.2 Powder XRD pattern of the $NiFe_2O_4$ calcinated at (a) 200, (b) 550 and (c) 500°C PDF Card No.:96-591-0065.

XRD was performed on the NFNPs/PVA Fig.3, it observations clearly indicate that the sample retained the spinel structure even after add PVA, where observed small intensity diffraction peaks at scattering angle 2θ=30.42 °, 35.79°, 37.463°, 43.501°, 54.18, 57.5°, and 63.108° may be assigned for X-ray scattering from the (220) (311) (222) (400) (422) (511) and (440), The intensities and positions of these peaks are in agreement with the literature [21].

The SEM images of $NiFe_2O_4$ annealed at 550°C are shown in Fig.4a,b.It is observed that, there is a uniform growth of nanocrystalline grains, and increase in porosity. formation of a well-defined, uniformly distributed and few sphere like structures

ISSN: 1813 – 1662 (Print)
E-ISSN: 2415 – 1726 (On Line)

were observed, $NiFe_2O_4$ shows the formation of honey comb like structure with large number of pores, due to gas release of combustion process[22] that the average size of the nanoparticles is about (42-29nm), which is larger than crystallite sizes determined by XRD patterns, thus it can be deduced that particles consist from individual crystallites.

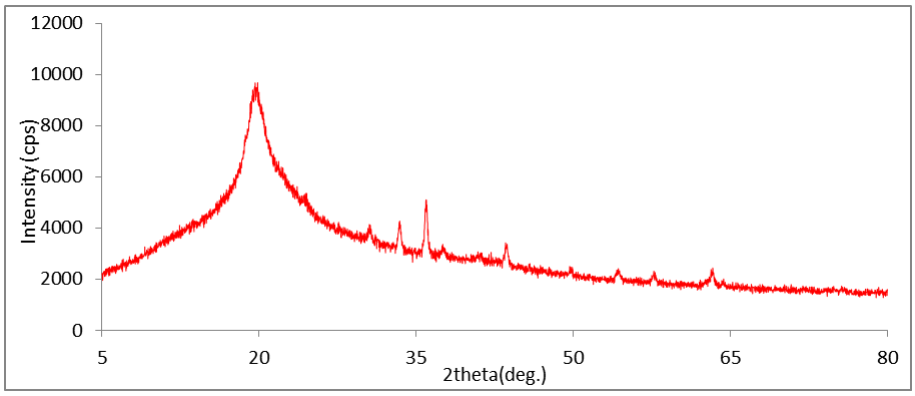

Fig.3 X-Ray Diffraction patterns of NFNPs/PVA nanocomposite.

Fig.4c shows an example of the scanning electron microscopy images of $NiFe_2O_4$/PVA polymer nanocomposite. A linear forked 3D structure indicate $NiFe_2O_4$ that shows almost homogeneous dispersion with some aggregation.

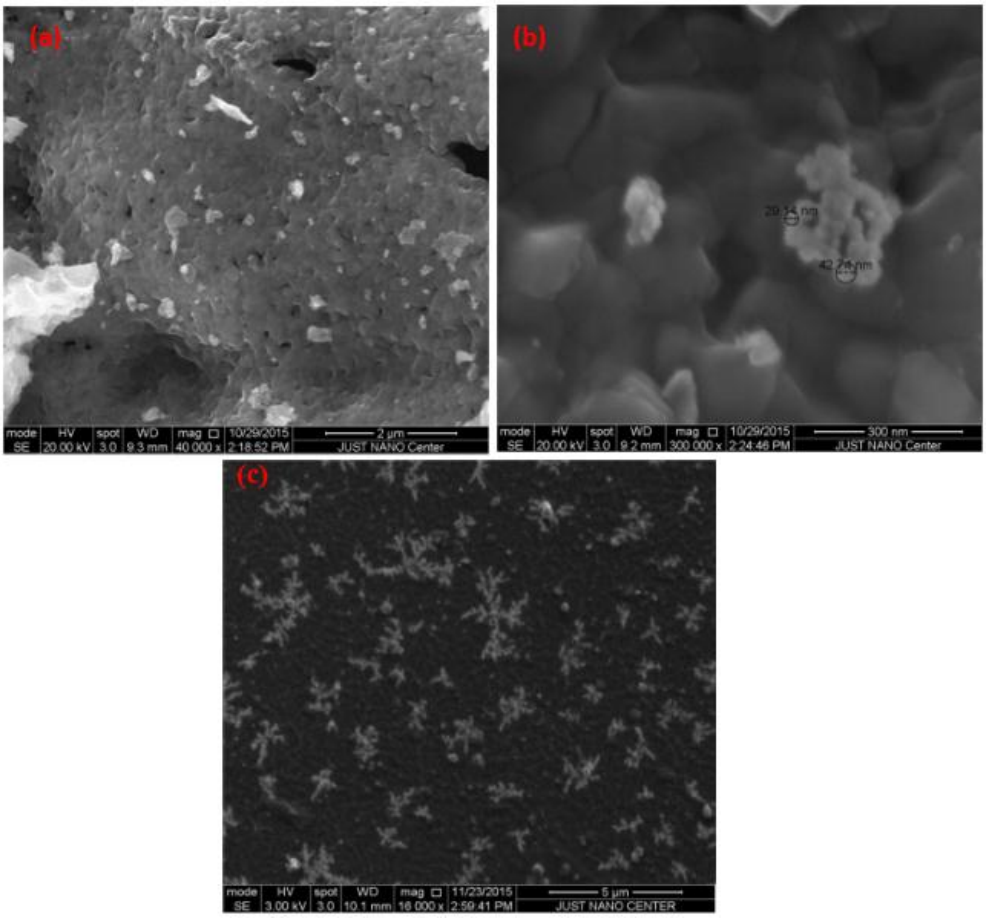

Fig.4 The SEM images (a) and (b) of NFNPs (c) of NFNPs /PVA matrix

Electrical Properties

The electrical measurements (dielectric permittivity , dielectric loss and conductivity) of PVA-NFNPs composites of different Nickel Ferrite contents were obtained at a frequency range from (5000Hz-1MHz) and at room temperature. The obtained results at room temperature are presented in Fig.5a-d A common feature can be seen in all the figures is that the addition of NFNPs increases the dielectric permittivity (ε'), dielectric loss(ε"), loss factor (tan δ) and conductivity (σ) of PVA host. Generally, NFNPs clearly enhances the electrical conductivity and the

polar character of PVA host. The variations of dielectric parameters with frequency can be explained in terms of the relaxation time; at low frequencies, the electric dipoles have sufficient time to align with the field before the field changes its direction; consequently the dielectric constant is high. At high frequencies, the dielectric constant value decreases due to the shorter time available for the dipoles to align [23]. The rise of conductivity with frequency which shown in Fig.5d, is common for polymeric and semiconductor samples [24]. As the dopant concentration is increased, the dopant molecules start bridging the gap separating the two localized states and lowering the potential barrier between them, thereby facilitating the transfer of charge carrier between two localized state [25].

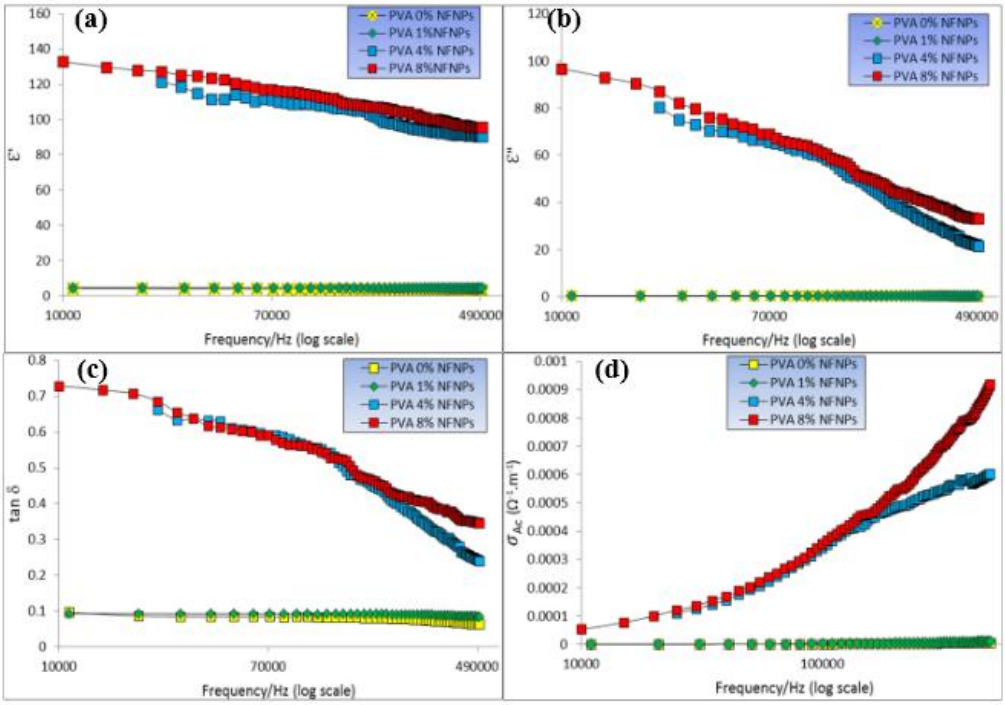

Fig.5 (a) Dielectric permittivity (ε') (b) imaginary permittivity (ε") (c) loss factor (tan δ) and (d) conductivity (σ) of the NFNPs/PVA composites with different consitration of NFNPs as a function of frequency at room temperature.

Conclusions

We have successfully synthesized high-performance NFNPs/PVA, nanocomposites by incorporating NFNPs into PVA aqueous solution. The synthesized composites exhibited a significant improvement in electrical properties at low loading of NFNPs compared to pure PVA. Moreover. NFNPs is an effective nanofiller, and can be used for many practical nanocomposites.

References

[1] C.R. Vestal, J.Z. Zhang, *Int. J. Nanotechnol.* 1 (2004) 240-263.

[2] J.-H. Lee, Y.-M. Huh, Y.-W. Jun, J.-W. Seo, J.-T. Jang, H.-T. Song, S. Kim, E.-J. Cho, H.-G. Yoon, J.-S. Suh, J. Cheon,. *Nat. Med.*, 13(2006) 95-99.

[3] C.B. Carter, M.G. Norton, *"Ceramic Materials: Science and Engineering"*, Springer (2007).

[4] Z.Ž. Lazarević, C. Jovalekić , A Milutinović , M.J. Romcević , A. Romcević, *Acta Physica Polonica*, 121(3) (2012) 682-686.

[5] H. Kavas, N. Kasapoğ lu, A. Baykal, *Chemical papers. Doi*, 10.2478/s. (2008) 6.

[6] R.K. Selvan, C.O. Augustin, L.J. Berchmans and R. Saraswathi, *Mater. Res. Bull.* 38 (2003) 41–54.

[7] M. Sultan and R. Singh, *Mater. Lett.* 63 (2009) 1764–1766.

[8] D. F. Zhao, H. Yang, R. S. Li, J. Y. Ma and W. J. Feng, *Materials Research Innovations*. 18,7 (2014) 520.

[9] S. Stankovich, D.A. Dikin, R.D. Piner, K.A. Kohlhaas, A. Kleinhammes, Y. Jia, Y. Wu, S.T. Nguyen, R.S. Ruoff, *Carbon*, 45 (2007) 1558-1565.

[10] K. Hung, C. S. Hsieh, W. D. Yang, H. Tsai, *J. Mater. Sci.* 33 (1998) 3721.

[11] V.A.M. Brabers, *Status Solidi* 33 (1969) 563–572.

[12] V. S. Bushkova, *International Science Index* 9 (2) (2015) 133-136.

[13] K.A. Rani, V.S. Kumar, *Int. J. of Adv. Sci. and Tech. Res.*, 6 (2014) 213-219

[14] R.D. Waldron, *Physical Review* 99 (1955)1727–1735.

[15] J.P. Singh, R.C. Srivastava, H.M. Agrawal, R.P.S. Kushwaha, *J. Hyperfine Interact.* 183 (2009) 393-400.
[16] P. Laokul, V. Amornkitbamrung, S. Seraphin, *Curr Appl Phy.* 11(2011) 101-108.
[17] M.G. Naseri, E.B. Saion, H.A. Ahangar, M. Hashim, A.H. Shaari, *Powder Technol*, 212 (2011) 80-88.
[18] Z. Yue, W. Guo, J. Zhou, Z. Gui, *J. Magn. Magn. Mater.* 270 (2004) 216-223.
[19] Z.H. Zhou, J.M. Xue, J. Wang, H.S.O. Chan, T. Yu, Z.X. Shen, *J. Appl. Phys.* 91, (2002) 6015-6021.
[20] K. Rafeekali, M. Maheem, E.M. Mohammed, *I.J.E.S.I.T.*, 4 (2015) 194-198.
[21] S. Sindhu, S. Jegadesan, A. Parthiban, S. Valiyaveettil, *Journal of Magnetism and Magnetic Materials* 296 (2006) 104-113.
[22] P. Priyadharshini, A. Pradeep, P.S. Rao, G. Chandrasekaran, *Mater. Chem. Phys.*, 116 (2009) 207.
[23] V. Raja, A.K. Sharma, V.V.R. Narasimha Rao, *Materials Letters*, 58 (2004) 3242-3247.
[24] M.H. Harun, E. Saion, A. Kassim, M.Y. Hussain, I.S. Mustafa, M.A.A. Omer, *Malaysian Polymer Journal*, l3 (2) (2008) 24-31.
[25] V.S. Sangawar, R.J. Dhokne, A.U. Ubale, P.S. Chikhalikar, S.D. Meshram, *Bull. Mater. Sci.*, 30 (2) (2007) 163-166.

تحضير المركب نيكل فرايت ($NiFe_2O_4$/PVA) ودراسة خصائصه الكهربائية

ابراهيم فهد وحيد[1] , عماد طه بكر[1] , صباح محمد علي[2]

[1]قسم الكيمياء ، كلية العلوم ، جامعة تكريت ، تكريت ، العراق

[2]قسم الفيزياء ، كلية التربية للعلوم الصرفة ، جامعة كركوك ، كركوك ، العراق

emaad_bakir@yahoo.com , imaofs83@yahoo.comsabah_yagmur@yahoo.com

الملخص

في هذا البحث ركزنا على تحضير مركب لاعضوي نانوي وهو Nickel Ferrite $NiFe_2O_4$ Nanoparticles (NFNPs) حيث يتم تحضير هذا المركب بطريقة الاحتراق الذاتي للسول–جل. مزج (NFNPs) مع متعدد (فينايل الكحول) (PVA) حيث نحصل على التركيب NFNPs/PVA وبنسب مختلفة من (NFNPs). شخص كل من PVA النقي والمركب NFNPs/PVA بتقنيات مختلفة بواسطة الاشعة تحت الحمراء (FTIR) والمجهر الالكتروني (SEM) وحيود الاشعة السينية للمسحوق (RXD). الصفات الكهربائية للمركب NFNPs/PVA درست حيث شملت السماحية الحقيقية (ε') والخيالية (ε"), والتوصيلية الكهربائية (σ_{Ac}) وعامل الخسارة (tan δ). حيث اجريت هذه القياسات في الترددات (5000Hz-1MHz) وفي درجة حرارة الغرفة.

كلمات البحث: نيكل فرايت, حيود الأشعة السينية (XRD), ثابت العزل الكهربائي.